

# Surface phase behavior in binary polymer mixtures. II. Surface enrichment from polyolefin blends

Frank Scheffold, Andrzej Budkowski,<sup>a)</sup> Ullrich Steiner, Erika Eiser, and Jacob Klein  
*Department of Materials and Interfaces, Weizmann Institute of Science, Rehovot 76100, Israel*

Lewis J. Fetters

*Exxon Research and Engineering Company, Annadale, New Jersey 08801*

(Received 18 December 1995; accepted 29 February 1996)

Using nuclear reaction analysis, we have measured the enrichment by one of the components at the surface of a binary mixture of random olefinic copolymers, with components of monomer structure  $E_{1-x_1}EE_{x_1}$  and  $E_{1-x_2}EE_{x_2}$ . Here  $E$  and  $EE$  are the linear ethylene and branched ethylethylene groups ( $C_4H_8$ ) and  $[C_2H_3(C_2H_5)]$ , respectively, and  $x$  represents the fraction of the  $EE$  group randomly distributed on the chains. We examined 12 different couples covering a range  $x=0.38$ – $0.97$ . The mixtures, whose thermodynamic behavior was established in our earlier paper, were cast in the form of films on both a silicon and on a gold-covered silicon surface, and were investigated in the one-phase region of the binodal in the vicinity of the critical temperature. We find that it is always the more flexible component—the one with a shorter statistical step length, corresponding to the higher ethylethylene fraction (higher  $x$ )—that is enriched at the polymer/air surface. Within our resolution neither component is enriched at the polymer/solid interface. These results show clearly that enthalpic rather than entropic factors dominate the surface potential driving the surface enrichment. For two of the mixtures we determined the excess of the surface-preferred species as a function of mixture composition along an isotherm in the one-phase region of the binodal. A consistent description of our data in terms of a mean-field model is provided by including in the surface potential a term in the mixture composition gradient at the polymer surface. © 1996 American Institute of Physics. [S0021-9606(96)51421-2]

## I. INTRODUCTION

The composition of surfaces exposed by polymer mixtures determines interfacial properties such as adhesion, frictional properties, wear resistance, and compatibility with adjacent phases. The surface of a binary mixture of partly miscible polymers  $A$  and  $B$  which favors one of the components will be enriched by that component,  $A$  say. When the mixture is in the two-phase regime, an  $A$ -rich phase  $\alpha$  will coexist with a  $B$ -rich phase  $\beta$  in the bulk and the  $A$ -favoring surface will be enriched in the  $\alpha$  phase. For the case of partial wetting, this enrichment will be limited to a finite, microscopically thin layer, while for complete wetting the  $\alpha$  phase will form a macroscopically thick layer, to the complete exclusion of the  $\beta$  phase.<sup>1–4</sup> These situations are shown schematically in Fig. 1 (and are clearly applicable to any binary mixture, not just polymers). Apart from their practical implications, there are important unresolved basic questions concerning surface enrichment or wetting from polymer mixtures. These include the issue of the partial-to-complete wetting transition on the bulk coexistence curve,<sup>5</sup> the order of the transition in such polymer mixtures, and indeed an understanding of the microstructural factors that drive either one or the other polymer to the surfaces. In addition, because of the experimentally convenient time and spatial dimensions associated with polymers at surfaces, they provide useful

models for studying more general structural and dynamic features of wetting.<sup>6</sup>

Theoretically, the question of wetting from binary polymer mixtures has been studied extensively in recent years. Nakanishi and Pincus<sup>7</sup> and Schmidt and Binder<sup>5</sup> extended to the case of polymers the earlier seminal discussion by Cahn<sup>1</sup> of wetting from simple liquid mixtures. Binder<sup>5,4</sup> has pointed out that complete wetting from coexisting polymer phases—in the sense described above and illustrated in Fig. 1(b)—should be possible even far below the bulk critical temperature  $T_c$ , in contrast to small molecule mixtures.<sup>1</sup> The underlying reason for this is the low translational entropy of bulk mixing of the flexible polymer chains, which derives from their large size. Such complete wetting on the coexistence curve was indeed observed in model polymer mixtures, at temperatures significantly below the bulk critical temperature.<sup>8,9</sup>

Earlier approaches emphasized the role of short-ranged enthalpic interactions in driving surface segregation and wetting from polymer mixtures.<sup>1,5</sup> More recent work has considered the effect of long-ranged van der Waals surface fields<sup>2,10,11</sup> and the role of entropic effects at impermeable surfaces.<sup>12–14</sup> A clear review of the theory has been presented by Binder.<sup>4</sup> In a recent analysis,<sup>15,14</sup> Fredrickson and Donley proposed that, in a binary polymer mixture, a potential of entropic origin would drive the more flexible chains to the surfaces. This is of interest in the context of the present work, where we study the surface behavior of a range of chemically similar chains of differing flexibility.

<sup>a)</sup>On leave from Jagellonian Univ., Krakow, Poland.

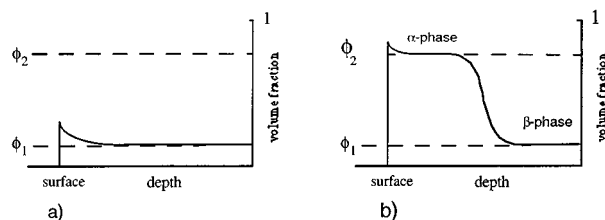


FIG. 1. Composition-depth profile near the surface of a binary  $A/B$  mixture at bulk concentration  $\phi_1$  of the  $A$ -poor phase  $\beta$ . (a) For the case of partial wetting the surface is covered by a microscopically thin layer enriched in the surface-preferred component  $A$ . (b) For complete wetting, a macroscopic layer of the  $A$ -rich  $\alpha$  phase forms at the surface to the complete exclusion of the  $\beta$  phase.

In recent years there have been a number of experimental studies of surface segregation and wetting from model binary polymer mixtures. These include mixtures of compatible<sup>16</sup> and of partly compatible polymers,<sup>17,18</sup> and isotopic mixtures of polymers and their deuterated counterparts.<sup>19,20</sup> In the latter it was found that the deuterated component was enriched at polymer/air and, often, at polymer/solid surfaces, driven there by a slight enthalpic preference. In our group we have carried out extensive studies of surface segregation from blends of polyolefinic copolymers.<sup>8,21,9</sup> These are random poly[ethylene ( $E$ )ethylethylene ( $EE$ )] copolymers of structure  $[(C_4H_8)_{1-x}-(C_2H_3(C_2H_5))_x]_N$ . They may be regarded as “effective homopolymers” whose mean microstructure  $E_{1-x}/EE_x$  varies continuously with  $x$  from polyethylene ( $x=0$ ) to poly(ethyl ethylene),  $x=1$ . Such mixtures, where the two components have  $EE$  fractions  $x_1$  and  $x_2$ , say, present an attractive model system, as in principle both the bulk and surface interactions may be tailored by suitable choice of the different  $x$  values. This enables a study of surface segregation effects as the microstructure of the mixture components is varied systematically, and forms the basis of the present investigation.

In the previous paper (I)<sup>22</sup> of this series we used nuclear reaction analysis (NRA) to examine in detail the miscibility, coexistence, and bulk interactions in 12 different, partly miscible  $E_{1-x}/EE_x$  mixtures covering a wide range of  $x$  values. In the present work we study equilibrium surface segregation from the same 12 blends, in the one-phase regime of the phase diagram. We examine in particular the correlation between surface enrichment and the chain microstructure of the mixture components, for both the polymer/air surface and for different polymer/solid surfaces. We then focus on the detailed surface excess isotherms from two of these mixtures, as the mixture composition in the one-phase region approaches the phase coexistence line. Our results are analyzed in terms of mean-field models, using the bulk interaction data obtained in I,<sup>22</sup> for a preliminary discussion of surface enrichment from such binary polymer blends. In a subsequent paper (Paper III) we extend our investigation to several different temperatures, allowing us to examine in detail the question of partial and complete wetting in these model mixtures.

TABLE I. Characteristics of the  $(E_{1-x}EE_x)_N$  polymers.  $x$  is the %  $EE$  (ethylethylene) monomer randomly distributed along each polymer backbone.  $N$  is the weight-averaged degree of polymerization (polydispersity index  $<1.08$  in all cases), and  $f_d$  is the fraction of hydrogen replaced by deuterium on the  $dx$  samples.

Sample $dx/hx$	$N$	$f_d$
$d38/h38$	1830	0.37
$d52/h52$	1510	0.34
$d66/h66$	2030	0.40
$d75/h75$	1625	0.40
$d86/h86$	1520	0.40
$d94/h94$	707	0.30
$d97A/h97A$	1600	0.35

## II. EXPERIMENT

$E_{1-x}/E_x$  random copolymers  $[(C_4H_8)_{1-x}-(C_2H_3(C_2H_5))_x]_N$  with seven different  $x$  values in the range 0.38–0.97 were used, giving—with their partly deuterated counterparts—14 different polymers in all. Their molecular characteristics are given in Table I. We note that (with the exception of the  $x=0.94$  copolymer) the degrees of polymerization are all in the range  $N=1750\pm 250$ , while the deuteration levels for the partly deuterated chains are also within a relatively narrow range  $f_d=0.35\pm 0.05$ . The statistical segment lengths  $a(x)$  of such copolymers, defined as  $a(x)=6R_g/N^{1/2}$ , where  $R_g$  is the unperturbed radius of gyration, decrease monotonically with increasing ethyl ethylene content  $x$ , as shown in Fig. 2. The critical temperatures for the 12  $dx_1/hx_2$  blends investigated in this study were determined in paper I<sup>22</sup> and are given in Table II.

Analytical grade toluene was used for the polymer solutions which were spin cast on silicon wafers to form thin films of the required copolymer mixtures. The films were in the thickness range 250–1200 nm, uniform to within a few nm over the area of the wafer. The polished silicon wafers

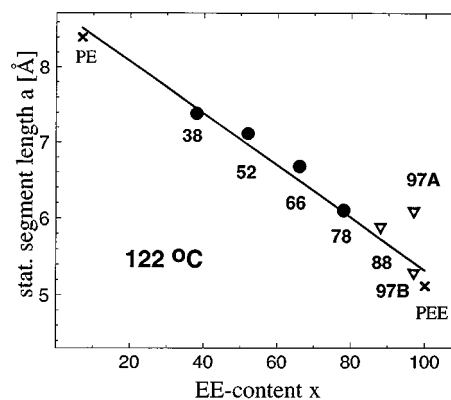


FIG. 2. Variation of the statistical segment length  $a(x)$  with percentage  $x$  of  $EE$  groups randomly distributed on the  $(E_{1-x}EE_x)_N$  backbones. The term  $a(x)$  is defined via the experimentally determined radius of gyration  $R_G(x, N)$  of the chain as  $R_G^2=Na(x)^2/6$ ,  $N$  being the respective degree of polymerization.  $\times$ —Balsara *et al.*, *Macromolecules* **25**, 6137 (1992);  $\bullet$ —Ref. 30;  $\nabla$ —Zirkel *et al.*, *Macromolecules* **25**, 954 (1992). The data is corrected to 122 °C.

TABLE II. Surface excess values from  $dx_i/hx_j$  mixtures.  $T_c$  and  $T_a$  are the bulk critical temperatures and the annealing temperatures of the mixtures, respectively.

$dxi/hxj$ mixture	$T_c$ [°C] <sup>a</sup>	$T_a$ [°C]	$\phi_x$ [%] <sup>b</sup>	Surface Excess $\Gamma$ [nm] air <sup>c</sup>	Surface Excess at Gold <sup>d</sup>	Surface Excess at Silicon <sup>d</sup>
<i>d52/h38</i>	77±7	74	17.9	9.3±0.9	No Enrich.	No Enrich.
<i>h52/d38</i>	50±10	40	19	-8.2±2.4	...	...
<i>d66/h52</i>	204±4	184	19.2	6.8±0.7	No Enrich.	No Enrich.
<i>h66/d52</i>	88±4	95	18.6	-10±2.6	...	...
<i>d75/h66</i>	101±4	99	18.6	4.6±0.4	No Enrich.	No Enrich.
<i>h75/d66</i>	33±10	40	19.6	-2.9±1.9	...	...
<i>d86/h75</i>	181±4	178	18.6	6.3±0.6	No Enrich.	No Enrich.
<i>h86/d75</i>	97±4	110	19.5	-4.7±2	...	...
<i>d94/h86</i>	50±6	40	20.0	2.9±0.3	No Enrich.	No Enrich.
<i>h94/d86</i>	<30	25	19.4	-5.2±2.1	...	...
<i>d97/h86</i>	223±5	172	17.3	5.2±0.5	No Enrich.	No Enrich.
<i>h97/d86</i>	75±10	40	19.6	-2.9±1.9	...	...

<sup>a</sup>Determined in paper I (Ref. 22).

<sup>b</sup>The bulk concentration  $\phi_x$  refers in all cases to the more highly branched component (higher  $x$ ).

<sup>c</sup>—Enrichment at the polymer/air surface by the higher branched components. Negative values of  $\Gamma$  imply evaluation of surface excess (of the higher branched components) through measurement of a depletion layer of the deuterated component.

<sup>d</sup>—“No enrichment” at the polymer/solid surfaces implies an enrichment (if any) lower than the experimental resolution  $\delta\Gamma = \pm 0.5$  nm. Dots (...) imply that no measurement was attempted.

(obtained from Aurel GmbH, Germany; orientation 1 0 0;  $p$  doped: resistivity 1–30  $\Omega$  cm) were either degreased in pure toluene (which leaves a thin SiO<sub>2</sub> layer on each wafer), or covered with an evaporated high-purity smooth gold layer (thickness  $\sim 20$  nm).

The samples (wafer size  $\sim 1 \times 1.5$  cm<sup>2</sup>) were annealed for times which varied with the annealing temperature, but were in all cases sufficient to ensure that the surface segregation had reached its equilibrium value. For temperatures above 70 °C, due to the high mobility of the model polyolefins used in this study, annealing times of less than a day or two were sufficient to reach steady state. In this temperature range the samples were either annealed in a high stability ( $\pm 1$  °C) vacuum oven ( $10^{-3}$  bar), or, at the highest temperatures, they were sealed in glass ampoules under vacuum ( $< 10^{-5}$  Torr) in order to prevent degradation. For temperatures below 70 °C the samples were sealed and annealed at normal pressure in a temperature stabilized liquid bath ( $\pm 0.2$  °C) or, at the lowest temperatures (25 °C) in a temperature stabilized room ( $\pm 0.5$  °C) for up to many weeks. After annealing the samples were quenched to a temperature below the glass transition temperature ( $< -80$  °C) and stored at this temperature until required for the NRA measurements. A jig was constructed which enabled the samples to be removed from the oven at the high annealing temperatures and to be projected rapidly into the quenching bath. This ensured very rapid cooling, and was done to eliminate as far as possible surface-nucleated spinodal decomposition during the cooling process.

After annealing, composition-depth profiles within the samples (normal to the film surface) were determined using NRA. In this method (which has been described in detail earlier<sup>23,24</sup>) a beam of energetic, charged <sup>3</sup>He particles is incident on the polymer film and reacts exothermically as



with the <sup>2</sup>H labels on the deuterated chains. The energy spectrum of the reaction products is detected and contains information on the depth at which the reaction took place. From this the composition-depth profile of deuterated segments is obtained directly. The spatial resolution of the method when detecting <sup>4</sup>He particles emitted in the forward direction depends on the incident energy of the <sup>3</sup>He beam and on the depth within the sample. It is highest at the sample surface. The technique (in the <sup>4</sup>He detection mode) yields a spatial resolution<sup>25</sup> of  $\sigma = 7$  nm at the polymer/air surface for an incoming <sup>3</sup>He energy of 700 keV (but the overall depth range is then limited to  $\sim 450$  nm) and stays better than approximately  $\sigma = 25$  nm for depths up to 600 nm for an incoming energy of 1.2 MeV (for which the overall depth range is  $\sim 1000$  nm.)

In all our earlier studies, <sup>4</sup>He particles were detected at a forward angle (see also preceding paper I<sup>22</sup>). In the present

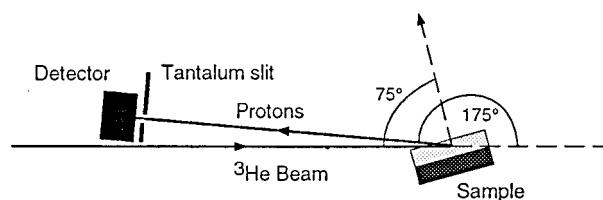


FIG. 3. Configuration for NRA of the reaction  ${}^3\text{He} + {}^2\text{H} \rightarrow {}^4\text{He} + {}^1\text{H}$  in the proton detection mode. In contrast to the <sup>4</sup>He detection mode at a forward grazing angle, there are no elastically backscattered <sup>3</sup>He particles in the energy range of interest, so that a magnetic deflection filter is unnecessary. The low angular dependence of the backscattered proton energies enable high reproducibility in the position of the polymer/air surface, and necessitate only a single slit as shown.<sup>27</sup>

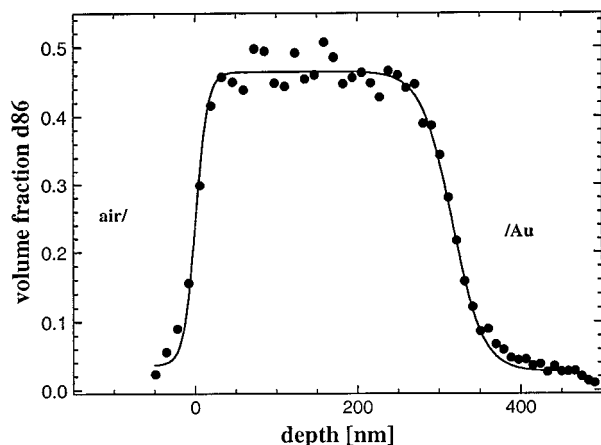


FIG. 4. Composition-depth profile of  $d86$  across a film of a  $d86/h86$  mixture. The 48.4%/51.6% mixture was annealed for 5 h at 120 °C. No surface excess is observed within the scatter at either surface.

investigation, for several of our samples, we detect rather the emitted protons ( $^1\text{H}$ ) in a backward direction. The geometry of this configuration is shown in Fig. 3. The main reason for this is that, due to the kinematics of the reaction (1), the energy of such backward emitted protons is far less sensitive to their angular spread when reaching the detector than is the case for forward emitted  $^4\text{He}$  particles.<sup>26,27</sup> This enables the position of zero depth ( $z=0$ , Fig. 3) to be determined with a reproducibility  $\pm 1$  nm, allowing an accurate determination not only of surface excess of deuterated segments but also of their depletion at the surface.

### III. RESULTS

Surface enrichment was studied from the 12 different  $dx_1/hx_2$  mixtures detailed in Table II (here  $d$  or  $h$  stand for partly deuterated or fully hydrogenated species, while  $x$  is in %). As a control we first checked for the effect of the isotopic differences alone. Figure 4 shows the composition-depth profile through an annealed film of a 50%/50%  $d86/h86$  mixture. The surface excess of deuterated segments at either surface is lower than our detection resolution, indicating that the driving force to the surface due to the deuterium labeling is not significant in our experiments.

Mixtures of the components at concentrations close to 20%/80% were prepared in toluene and spin cast from the solution onto silicon wafers to create films of uniform thickness in the range 250–450 nm. These values are much larger than the bulk correlation lengths or the characteristic decay lengths of the surface enrichment peaks (20–30 nm), or of the typical gyration radii (10 nm), so that finite size effects on the surface enrichment are expected to be small.<sup>20,28</sup> At the same time the films are thin enough to enable NRA to probe mixture compositions with good resolution (using a 700 keV incident  $^3\text{He}$  beam and detecting emitted  $^4\text{He}$  in the forward direction), not only at the air but also at the solid substrate surface. In all mixtures, the 20% component was the one with the higher  $EE$  fraction  $x$ .

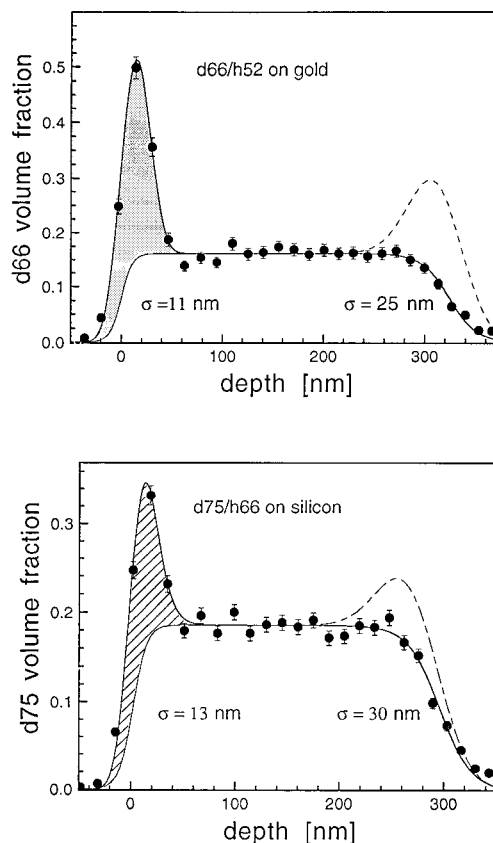


FIG. 5. Typical composition-depth profiles through annealed films of  $dx_1/hx_2$  mixtures, for  $x_1 > x_2$ . (a) Profile of a 20%  $d66/80\%$   $h52$  blend annealed for 2 h at 168 °C on a gold-covered substrate. (b) Profile of a 20%  $d75/80\%$   $h66$  blend annealed for seven days at 60 °C on a bare silicon substrate. Clear surface excess peaks  $\Gamma$  (air) of the  $dx_1$  component are observed at the air surface (shaded), while no corresponding peaks are detected—within the NRA resolution—at either solid surface. For contrast, broken curves show the signal at the polymer/solid interface that would be expected for a surface excess equivalent to  $\Gamma$ (air) [ $\sigma$  represents the spatial resolution at the respective surfaces.<sup>25</sup>]

Samples were annealed at temperatures  $T_a$  near or above the critical temperatures  $T_c$  in all cases, as given in Table II, to ensure that the 20%/80% compositions were within the one-phase regime and well away from the binodal. Following annealing to equilibrium the films were rapidly quenched and stored at temperatures below their  $T_g$ ; subsequently they were mounted in the scattering chamber and the composition-depth profile of the deuterated segments determined via NRA.

Two types of composition depth profiles were observed. In mixtures where the deuterium label was on the component with the higher branched content, a marked peak in the deuterated segment fraction was clearly observed at the polymer/air interface, corresponding to enrichment at this surface of the higher  $x$  component. Typical profiles of this sort are shown in Figs. 5(a) and 5(b) [for  $d66/h52$  and  $d75/h66$ , respectively]. We examined such profiles carefully for the presence of a surface excess peak at the polymer/solid interface, by using films at the lower end of the thickness range (down to 250 nm) in order to improve the resolution at this interface. We found that for all six mixtures where the more

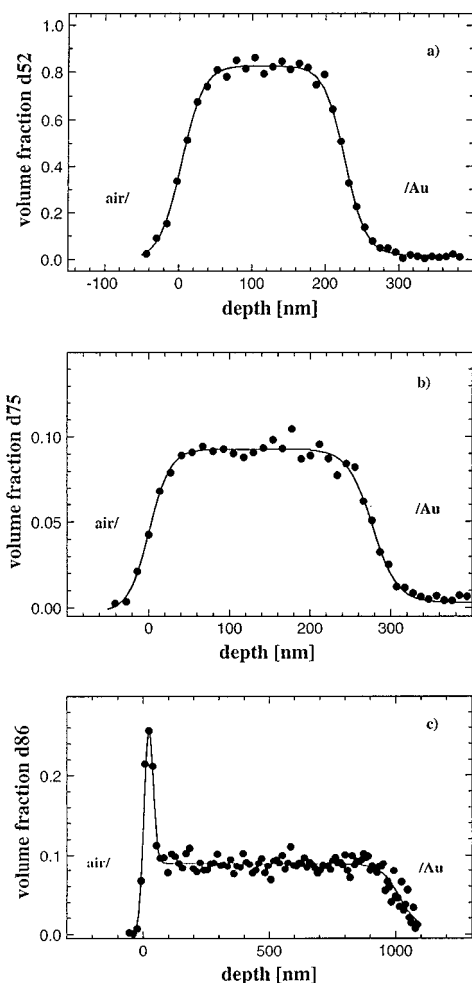


FIG. 6. Composition-depth profiles through annealed films of  $hx_1/dx_2$  mixtures, for  $x_1 > x_2$ . (a) Profile of an 20% $h66/80\%$  $d52$  film annealed for 43 h at 72 °C [this is the same mixture composition shown in Fig. 5(a) but with the deuterium label exchanged]. (b) Profile of a 90.5% $h86/9.5\%$  $d75$  film annealed for 4.5 h at 112 °C. Within the NRA resolution, no surface excess peaks of the deuterated component are observed at either air or solid interface in either (a) or (b). To contrast with (b), the profile in (c) is for a film of composition 9.6% $d86/90.4\%$  $h75$  annealed for 4.5 h at 112 °C: here the higher  $x$  component is deuterated and a clear air surface excess peak is observed, consistent with the profiles of Fig. 5.

branched component was deuterated there was a clear absence of a peak at the solid surface, for both the bare silicon surface and for the gold-coated wafers, as typified in Figs. 5(a) [gold covered] and 5(b) [bare silicon]. That is, within our resolution  $\delta\Gamma \approx \pm 0.5$  nm in determining the surface excess  $\Gamma$ , no enrichment of the higher  $x$  component could be detected at either polymer/solid interface. For comparison, we show in these figures—as a broken curve—how a surface excess at the polymer/solid interface would have appeared for the same  $\Gamma$  values corresponding to the peak at the polymer/air surface.

For the couples where the deuterium label was on the component with the lower  $x$  value, no surface excess of the deuterated segments was observed at either the polymer/air or the polymer/solid surfaces. A typical profile is shown in Fig. 6(a) [for 20% $h66/80\%$  $d52$  couple]. A more direct con-

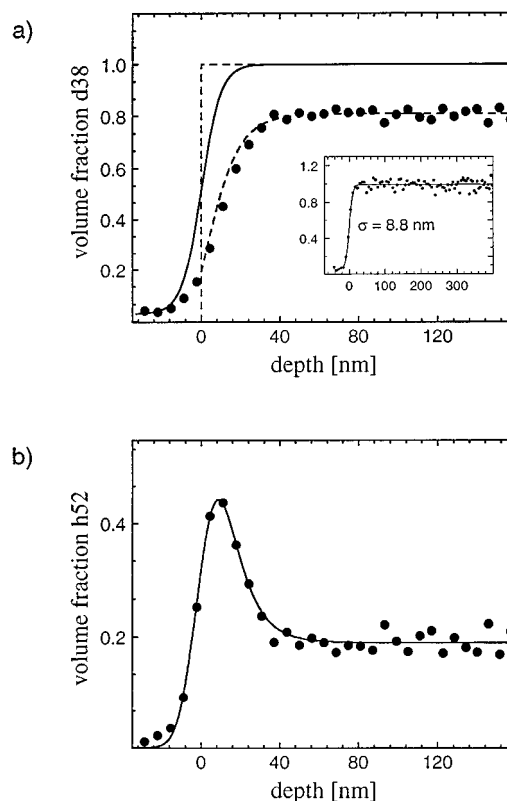


FIG. 7. Illustrating the extraction of surface excess of  $hx_1$  from concentration-depth profiles of films of  $hx_1/dx_2$ , where  $x_1 > x_2$ . The procedure converts the concentration vs depth profile of the deuterated component (which is depleted at the air surface) to a concentration vs depth profile of the nondeuterated component. (a) shows the original spectrum of a 20%  $h52/d38$  blend annealed at 40 °C and a tanh fit to a profile of a deuterated layer with volume fraction  $\phi=1$ , based on a profile of a fully deuterated film as shown in the inset ( $\sigma$  is the resolution half width). (b) after subtraction of the tanh fit, a concentration vs depth profile of the nondeuterated component  $h52$  is obtained.

trast illustrating the difference between the low and high  $x$  components is shown in Figs. 6(b) and 6(c) for couples where the deuterated species were at low concentrations. For the mixture 10% $d75/90\%$  $h86$  [Fig. 6(b)] we find—within our resolution—no enrichment of the deuterated species at either interface, while an annealed 10% $d86/90\%$  $h75$  profile shows the clear enrichment expected of the  $d86$  component at the air surface, [Fig. 6(c)]. The mixtures were annealed at 112 °C, well in the one-phase region for both mixtures at these concentrations.

We investigated the enrichment at the air surface by the more highly branched chains from mixtures where they did *not* carry the deuterium label. This involved measuring whether the deuterated (less branched) chains were in fact *depleted* at the polymer/air interface. This is a less straightforward procedure than for the case of a deuterated surface excess (as, for example, in Fig. 5), and was carried out as illustrated in Fig. 7. A composition-depth profile of a film consisting only of deuterated polymer was fitted to a step function convoluted with the system resolution, and the composition then normalized to 1, as shown in the inset and the solid curve in Fig. 7(a). The profile of the the

$dx_1/hx_2(x_1 < x_2)$  mixture following annealing was then measured, and normalized to its bulk volume fraction [data points in figure 7(a)]. Subtraction of the mixture profile from the fit to the (deuterated) single-component profile yields the corresponding composition-depth profile of the hydrogenated component  $hx_2$  as shown in Fig. 7(b). This reveals the clear surface enrichment peak of the hydrogenated copolymer, i.e., the component with the higher ethyl-branching ratio. We emphasize that this procedure is only possible using NRA in the proton-detection mode noted earlier: it is the reproducibility in the location of the polymer/air interface ( $\pm 1$  nm) which enables the difference between the  $^1\text{H}$ -enriched profiles and the control fully deuterated layer to be determined with the necessary accuracy within a given set of runs. We note that the same procedure cannot be applied at the much deeper polymer/solid interface: this is because the precise position of this interface is not known with sufficient accuracy, and also due to insufficient resolution at that depth even for the thinnest films used ( $\sim 250$  nm).

Integral surface excess values  $\Gamma = \int_{z=0}^{z_\infty} (\phi(z) - \phi_\infty) dz$ , where  $\phi_\infty$  is the plateau value of the mixture composition and  $z_\infty$  is depth at which  $\phi(z) = \phi_\infty$ , were determined from peaks such as in Fig. 5 or in Fig. 7(b), for all 12 mixtures<sup>29</sup> (due account being taken of finite resolution, see caption to Fig. 9). The normalization to absolute volume fraction values is carried out by equating the integrated amount of deuterated segments in each profile to the known overall amount of such segments in the film. The values for the surface excess of the deuterated (positive values of  $\Gamma$ ) or the hydrogenated (negative values of  $\Gamma$ ) component are listed in Table II. Clearly, in all cases it is the more highly branched component that is enriched at the air surface when the mixtures are at equilibrium in the one-phase region of the coexistence space; this is irrespective of which of the components carries the deuterium label. There is no enrichment (within our resolution) by either component at the solid surfaces.

A second set of samples was prepared for two of the mixtures, *d66/h52* and *d94/h86*, for a systematic study of the surface excess isotherms. For these, thicker films (in the range 600–1000 nm) were spin cast onto gold-covered silicon wafers, at several compositions in the range 2%–40% of the deuterated component. The thicker films were cast in order to ensure that finite size effects were quite negligible. The phase coexistence diagrams of these blends were determined separately in our earlier study (paper I) and are reproduced in Figs. 8(a) and 8(b), together with the different bulk compositions studied (marked  $\blacktriangle$ ) along the isotherms at the annealing temperatures for each sample. The temperatures chosen, 184° and 40 °C for the *d66/h52* and *d94/h86* mixtures, respectively, were selected to be some 10–15° below the respective critical temperatures, and the highest mixture compositions examined were close to the binodal line but still in the one-phase region (Fig. 8). Clear surface enrichment peaks of the deuterated components (i.e., *d66* and *d94*, respectively) were observed for all compositions at the polymer/air interface (see, e.g., Fig. 9) and the surface excess values—which increased monotonically with increasing volume fraction of the more branched components—were mea-

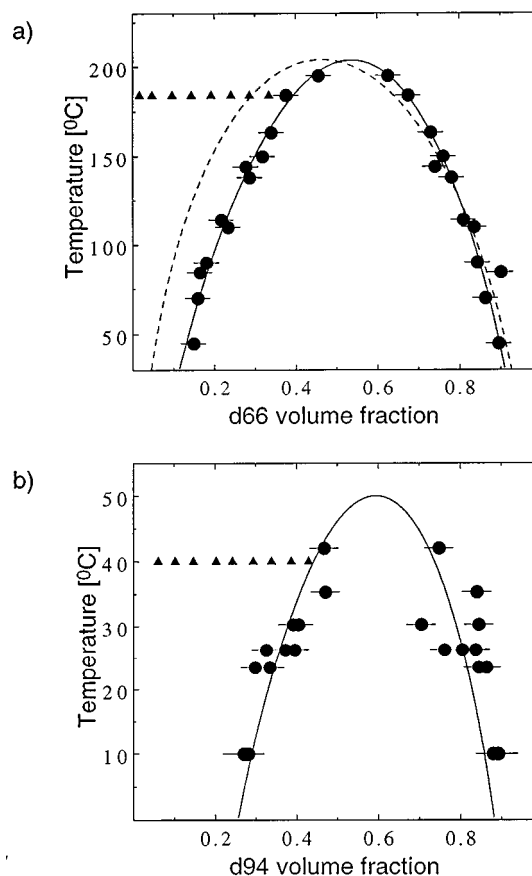


FIG. 8. Phase coexistence diagrams for the binary mixtures (a) *d66/h52* and (b) *d94/h86*, taken from paper I.<sup>22</sup> The solid lines are based on the Flory–Huggins model with segmental interaction parameters as follows ( $\phi$  is the volume fraction of deuterated component):

$$(a) \text{ } d66/h52: \chi(T, \phi) = (0.324/T + 3.48 \cdot 10^{-4}) \cdot (1 + 0.222 \cdot \phi)$$

$$(b) \text{ } d94/h86: \chi(T) = (0.647/T).$$

The broken curve in (a) is based on the composition-independent form  $\chi(T) = (0.548/T)$  for the interaction parameter of the *d66/h52* mixture. Compositions along the 184 °C and 40 °C isotherms in the one-phase region, where surface excess values were measured for the two mixtures, are shown as  $\blacktriangle$ .

sured as described above. These are given in Table III and plotted in Figs. 10 and 11. For these thicker samples the resolution at the polymer/gold interface was poorer than for the thinner films used in the first part of our study, and the question of surface segregation at the solid surfaces was not examined.

## IV. DISCUSSION

### A. Enthalpically driven vs entropically driven surface enrichment

A central finding of the present study is that in mixtures of  $E_{1-x}E_x$  copolymers in the miscible (one-phase) regime it is the component with the higher ethyl branching fraction (higher  $x$ ) that is preferentially adsorbed at the polymer/air surface. At the same time we find no evidence within our resolution of enrichment by either component at the polymer/solid interface, at the mixture compositions studied.

What is the origin of this behavior? The isotopic factor, which in certain cases can drive surface segregation of the

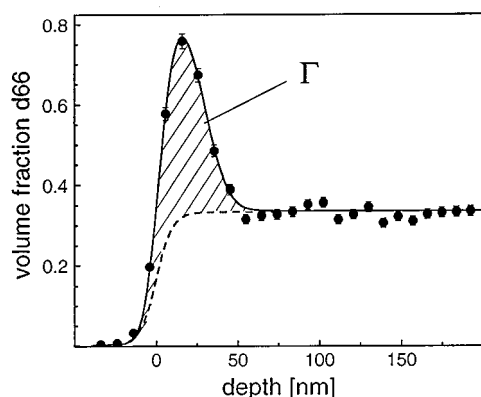


FIG. 9. Concentration-depth spectra of a 35% *d66/h52* blend annealed at 184 °C. A clear enrichment of the deuterated component *d66* at the free surface is observed. The integral surface excess  $\Gamma$  is evaluated by fitting the peak with an appropriate top hat function convoluted with the system resolution at the surface. Subtraction of a top hat-profile convoluted with the system resolution, (dashed line), yields the integral surface excess as the shaded area (use of a convoluted truncated tanh profile for the surface peak made little difference to  $\Gamma$ ).

deuterated species from deuterated/protonated mixtures,<sup>19,20</sup> can be ruled out at once. We note that any preferential surface interaction provided by the deuterium label alone is too small to lead to a detectable surface excess even for an isotopic mixture of identically branched components (see Fig. 4), while for different branching ratios it is always the more branched component that segregates to the air interface, irrespective of the deuterium labeling.

Generally in a binary mixture it is the component with the lower surface energy that is expected to be enriched at that surface. Since the differences in the chemistry of the two components in the  $E_{1-x}EE_x$  mixtures studied are slight (both monomer types being isomers of  $(C_4H_8)$ , and differing relatively slightly in the extent,  $x$  of ethyl branching) we expect, *a priori*, little chemical driving force for such an enrichment. Nonetheless, there are reasons to expect a preference for the more branched chains at a surface on purely enthalpic grounds. Bulk PVT studies of melts of  $E_{1-x}EE_x$  random copolymers suggest that the higher branched materials have lower cohesive energies.<sup>30</sup> This in turn implies a lower energy per unit area of exposed surface, and favors surface enrichment. The effect would be strongest at an air or vacuum surface, where there are no compensating interactions, and would be weaker at a polymer/solid interface where interactions with the surface atoms of the solid would act to partially compensate for the loss of interactions relative to a free surface. This is consistent with our observations that the higher ethyl-branched components are enriched at the air surface but not (within our resolution) at the solid surface.

At a qualitative level the origin of the lower cohesive energies in the higher branched polyolefin may be argued as follows: the statistical segment length of such molecules decreases monotonically with increased branching, i.e., higher  $x$  values, as in Fig. 1. Thus the higher- $x$  copolymers have shorter and thicker segments, and in a given volume these segments will have more self-interactions with other seg-

TABLE III. Polymer/air surface excess values for the *d66/h52* and *d94/h86* couples.

$\phi_x$ , %	<i>d66/h52</i> , 184 °C	
	$\Gamma$ (nm)	$\pm$ (nm)
1.7	1.45	0.38
4.6	3.25	0.47
4.7	2.25	0.32
9.6	4.62	0.51
14.3	6.28	0.63
14.3	6.07	0.61
19.2	7.10	0.68
19.2	6.50	0.62
24.0	8.49	0.79
24.0	8.49	0.79
28.6	9.87	0.89
28.5	10.9	0.99
33.6	11.6	1.0
33.1	14.3	1.3
	<i>d94/h86</i> , 40 °C	
6.0	1.28	0.17
6.0	1.25	0.16
10.1	1.48	0.16
10.1	1.51	0.17
14.6	2.02	0.20
14.6	2.72	0.27
20.0	2.97	0.28
20.0	2.97	0.28
24.1	4.16	0.38
24.4	3.03	0.28
29.4	4.59	0.41
29.1	5.53	0.50
33.9	4.34	0.39
33.7	5.26	0.47
38.6	7.24	0.64
38.9	5.91	0.52
42.8	14.2	1.2
43.0	13.1	1.1

The plateau composition values are of the deuterated components (*d66* or *d94*). The third column for each couple gives the estimated uncertainties in  $\Gamma$ .

ments of the same chain and fewer with segments from other chains. Since it is the latter which are responsible for the cohesion of the material, higher branching ratios are expected to be correlated with lower cohesive energies, as suggested by the bulk studies.<sup>30</sup> Extending the argument to interfaces, one may say that—per unit area of a free surface—the shorter, thicker segments are expected to lose fewer interactions with segments in the half space of the bulk (“missing neighbor” effect) than would longer, thinner segments: thus the surface enrichment of such segments would be associated with a lower surface energy. The argument assumes that short-ranged forces dominate the surface interactions.

The possibility that it is entropic rather than enthalpic factors that prove the driving force to interfaces from mixtures of different polymers has recently been considered by Cohen and Muthukumar<sup>12</sup> and by Fredrickson and Donley.<sup>13,14</sup> In both cases the idea is that in the vicinity of an impermeable surface there are restrictions on the configurations of the polymers which modify the surface potentials differently for the different components of the binary mix-

ture. The leading additional term in the surface energies due to these modifications of entropic origin is proportional to the *gradient* of the composition at the surface,

$$\left. \frac{d\phi(z)}{dz} \right|_{z=0}.$$

In the Cohen–Muthukumar<sup>12</sup> approach the differences in this entropic factor for the two components are a function of the different binding potentials between the surface and the respective monomers.

The Fredrickson–Donley model,<sup>13</sup> on the other hand, considers the case where the two polymers have different statistical (Kuhn) segment lengths  $a_i$  and  $a_j$ . Using a density functional approach, they derive an expression for the entropic surface potential  $F_s^{ent}$  whose leading term in the long-wavelength limit is given by

$$F_s^{ent} = - (1/12)(a_i^2 - a_j^2)(d\phi/dz)_{z=0}. \quad (2)$$

This surface term, when acting alone, tends to favor an enrichment of the *more flexible* (shorter statistical segment length) component at the surface of the mixture. In general, however, it must be added to the more conventional surface interaction terms of enthalpic origin<sup>4</sup> to give the overall surface interaction energy. Clearly, the entropic surface potential  $F_s^{ent}$  will be most significant where the chemical differences between the two polymers in a binary mixture are least, so that surface energy differences of enthalpic origin are minimized. Mixtures of random polyolefinic copolymers of structure  $E_{1-x}EE_x$  used in the present study are thus, on the face of it, good candidates to examine this idea of an entropic driving force, especially where the values of  $x$  do not differ too greatly between the component chains. Indeed, in their original paper<sup>13</sup> Fredrickson and Donley suggest the use of polyolefin mixtures as optimal candidates for testing their model. Earlier studies of diblock copolymers,<sup>31</sup> where lamellae of the more flexible block always formed at both air and solid surfaces, were cited in support of this idea of an entropic driving force for surface segregation: more recent work,<sup>32</sup> however, suggests the Fredrickson–Donley model, explicitly developed for homopolymers, may not apply to diblocks.

It is thus of interest to examine this question in the light of our present results for random copolymers. The entropic effect described by Eq. (2) depends only on having the polymer mixture in the vicinity of an impermeable surface, and thus should apply equally well for our samples at both the air and the solid surfaces. While we do observe that the more flexible chains are always the ones enriched at the air surface, as might be expected on enthalpic grounds and is also predicted on the basis of Eq. (2), there is no corresponding enrichment (of either component, within our resolution) at the polymer/solid surface. Since the entropic driving force is the same for both surfaces, but leads to no enrichment at the solid surface (see, e.g., Fig. 5 or Table II), we must conclude that it plays little role in leading to the enrichment at the air surface. This implies that the magnitude of such an effect—even in an apparently optimal system such as ours—is much

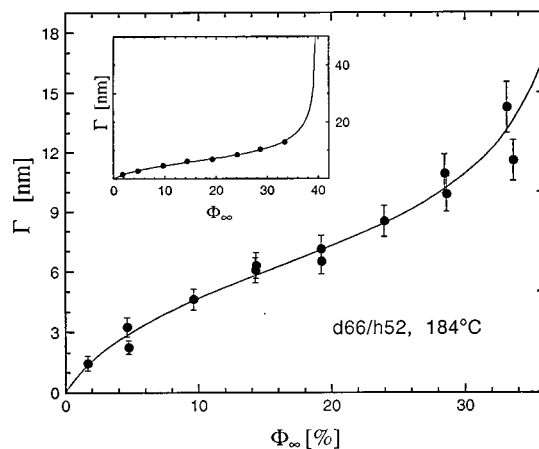


FIG. 10. Integral surface excess  $\Gamma$  vs bulk concentration  $\phi_\infty$  at 184 °C for the  $d66/h52$  mixture. The solid lines are calculated from a mean-field model assuming a composition gradient term in the surface potential [see text following Eq. (11)]. The inset shows the divergence of  $\Gamma(\phi_\infty)$  for  $\phi_\infty$  approaching the coexisting concentrations predicted by this fit.

smaller than any enthalpic contribution to the surface enrichment. Such a possibility was indeed raised in the original model by the authors themselves.<sup>13,33</sup> We conclude that the segregation of the more highly branched chains to the air surface is driven mainly by enthalpic factors as discussed above. At the same time, the apparent absence of any (or the presence of undetectably little) preferential segregation to the solid surface must be the result of a compensation of these enthalpic effects, due to interactions of the polymer segments with the surface atoms. An additional factor which may play a role is short-ranged layering (extending to one or two layers) of polymer segments at the smooth, impermeable solid interface<sup>34</sup> (but not at the more flexible air interface). This could favor the presence of the less-branched (i.e., more linear) chains, since such stiffer and more linear chains might be expected to layer more readily at the solid interface. Any such effect would offset the unfavorable entropic surface fields experienced by these less flexible chains.

## B. Surface enrichment and bulk interactions

We consider now in more detail the changes in the surface excess and in the surface concentration as the compositions vary along the isotherm in the one-phase region for two of the mixtures (Fig. 8). These surface excess isotherms—shown in Figs. 10 and 11 for the  $d66/h52$  and  $d94/h86$  blends, respectively—contain information on the surface interaction parameters and provide some preliminary insight on the nature of the surface enrichment. A good starting point for a mean-field description of the surface composition an  $A/B$  binary polymer mixture is the expression for the excess free energy  $\Delta F$  per unit area of surface due to the presence of one of the components ( $A$ , say) at volume fraction  $\phi(z)$  a distance  $z$  from the surface at  $z=0$ ,

$$\begin{aligned} \frac{\Delta F}{k_B T} = & f_s(\phi_s) + \int_0^\infty dz \left[ F_{FH}(\phi) - (\Delta\mu)\phi \right. \\ & \left. + \frac{a(\phi)^2}{36\phi(1-\phi)} \left[ \frac{d\phi}{dz} \right]^2 \right]. \end{aligned} \quad (3)$$

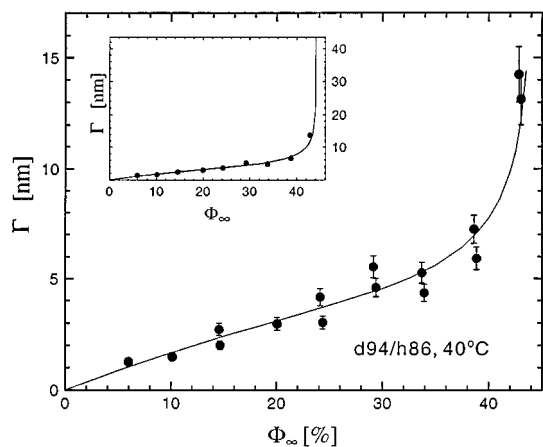


FIG. 11. Integral surface excess  $\Gamma$  vs bulk concentration  $\phi_\infty$  at 40 °C for the *d94/h86* mixture. The solid lines are calculated from a mean-field model assuming a composition gradient term in the surface potential [see text following Eq. (11)]. The inset shows the divergence of  $\Gamma(\phi_\infty)$  for  $\phi_\infty$  approaching the coexisting concentrations predicted by this fit.

This expression is based on an approach earlier described by Cahn<sup>1</sup> to discuss wetting from binary liquid mixtures, and extended to polymers at interfaces by de Gennes<sup>35</sup> and others.<sup>7,5</sup> The first term on the right-hand side (RHS) is the “bare” surface interaction term, assumed short ranged in the sense that it is a function of the surface concentration  $\phi_s [= \phi(z=0)]$  alone. The integral represents the free energy excess due to the composition profile  $\phi(z)$ . In this expression  $F_{\text{FH}}$  is the normalized Flory–Huggins free energy of mixing,<sup>36</sup> given by

$$F_{\text{FH}}/k_B T = (\phi/N_A) \ln \phi + [(1-\phi)/N_B] \ln(1-\phi) + \chi \phi(1-\phi), \quad (4)$$

where  $\chi$  is the segment interaction parameter.

The chemical potential difference between the two components is given by  $\Delta\mu[\partial F_{\text{FH}}/\partial\phi]_{\phi_\infty}$  and  $a(\phi) = \sqrt{(1-\phi)a_A^2 + \phi a_B^2}$  is a weighted statistical segment length (with statistical segment lengths of the pure components  $a_i$  defined via the radius of gyration  $R_G^2 = N_i a_i^2/6$  for each component  $i$ ). In our case the *A* and *B* chains are the *E/EE* copolymers, labeled by the respective *EE* fractions  $x_i$ . The values for  $a_{xi}$  used in the following calculations were interpolated from those given in Fig. 2 (and corrected for temperature dependence).<sup>30</sup>

We follow the standard procedure leading to the “Cahn construction” for discussing the surface enrichment properties.<sup>1</sup> Minimizing the free energy  $\Delta F$  [Eq. (3)] yields an expression for the derivative of the surface free energy  $f_s$  which depends only on the surface volume fraction  $\phi_s$  and on the bulk interactions

$$-\frac{df_s(\phi_s)}{d\phi_s} = \pm f_1(\phi_s), \quad (5)$$

where the function  $f_1(\phi_s)$  is given by

$$f_1(\phi_s) = \frac{a(\phi_s)}{3} \times \sqrt{\frac{F_{\text{FH}}(\phi_s, \chi) - F_{\text{FH}}(\phi_\infty, \chi) - \Delta\mu(\phi_s - \phi_\infty)}{\phi_s(1-\phi_s)}} \quad (6)$$

and  $\phi_\infty$  is the bulk volume fraction (e.g., the plateau composition in Figs. 5 or 7).

If Eq. (5) is solved by different values of  $\phi_s$  the solution yielding the minimum of the surface excess free energy  $F_s$  per unit area

$$\frac{F_s}{k_B T} = \int_{\phi_s}^{\phi_\infty} d\phi \left\{ -\frac{df_s(\phi)}{d\phi} + f_1(\phi) \right\} \quad (7)$$

is the physically correct one.

A crucial point for this discussion concerns the precise variation of the *bulk* free energy, essentially the Flory–Huggins interaction parameter  $\chi(T, \phi)$ . This was determined independently in our earlier study (paper I<sup>22</sup>) via determination of the binodals shown in Fig. 8, and the relevant values of  $\chi(T, \phi)$  are given in the caption to Fig. 8. In order to evaluate the surface free energy we make use of Eq. (5). Due to limited resolution of the NRA it is difficult to obtain the surface volume fraction  $\phi_s$  directly. However, the expression for the integral surface excess  $\Gamma$ , given by

$$\Gamma = \int_0^\infty (\phi(z) - \phi_\infty) dz = \frac{1}{6} \int_{\phi_\infty}^{\phi_s} \frac{a(\phi)(\phi - \phi_\infty) d\phi}{\sqrt{\phi(1-\phi)[F_{\text{FH}}(\phi) - F_{\text{FH}}(\phi_\infty) - \Delta\mu(\phi - \phi_s)]}} \quad (8)$$

contains  $\phi_s$  as the only unknown on the RHS. Since  $\Gamma$  is experimentally determined (see Figs. 10 and 11), the surface volume fraction  $\phi_s$  is readily evaluated numerically.<sup>37</sup> Figures 12(a) and 12(b) show the values of  $\phi_s$  obtained by this method for the *d66/h52* and *d94/h86* blends. Mean values for each concentration are displayed in order to reduce scatter. Using the values of  $\phi_s$  obtained in this way it is now possible to calculate the derivative of the surface free energy  $df_s/d\phi_s$ . These are shown in Figs. 13(a) and 13(b); also plotted in Fig. 13 (as broken curves) are the values of  $f_1(\phi_s)$  [Eq. 6] for the two mixtures at the respective temperatures, using the Flory–Huggins free energy expression with the appropriate values of the segment interaction parameter  $\chi(T, \phi)$  determined in paper I. The values of  $\phi_\infty$  are set at  $\phi_1$ , the coexistence compositions at the temperatures for which the surface excess values were determined for the respective mixtures. We emphasize the importance of using the form of  $\chi(T, \phi)$  which correctly describes (paper I<sup>22</sup>) the experimentally determined binodals. For example, use of the simpler form  $\chi(T) = A/T$  for the case of the *d66/h52* mixture would result in a binodal [broken curve in Fig. 8(a)] which predicts—wrongly—that the two highest compositions studied at 184 °C are within the two-phase regime.

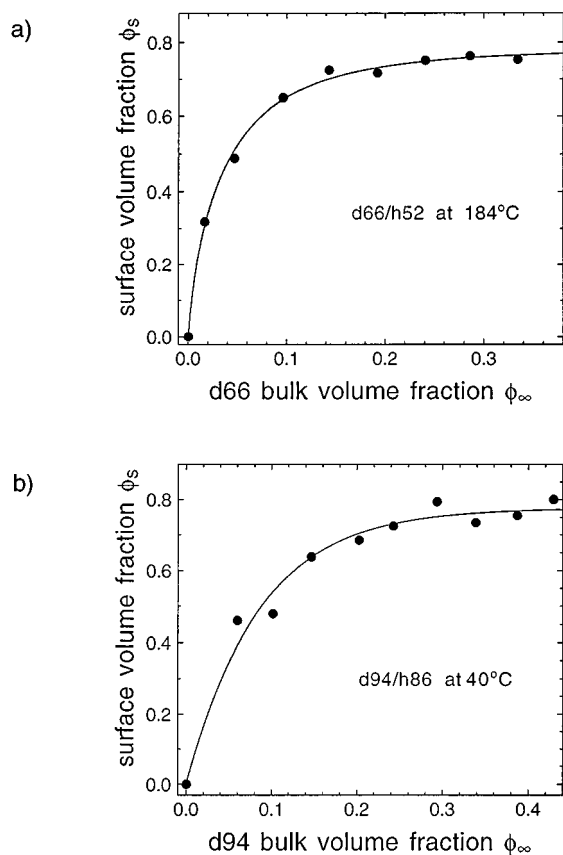


FIG. 12. Surface volume fraction  $\phi_s$  as a function of  $\phi_\infty$  obtained from the integral surface excess  $\Gamma$  using Eq. (8). (a) *d66/h52* at 184 °C. (b) *d94/h86* at 40 °C. The solid lines are calculated from a mean-field model assuming a composition gradient term in the surface potential [see text following Eq. (11)].

### C. The nature of the enrichment layer

Figure 13 shows the so-called Cahn construction for the two mixtures studied: this construction enables a graphical solution of Eq. (5), and allows us to determine the nature of the enrichment by the surface-preferred component at the polymer-air surface. Whether, at the coexistence composition, one expects a partial wetting layer, as in Fig. 1(a), or complete wetting as in Fig. 1(b), can be discussed on the basis of Eqs. (5) and (7). The intersections of the data points representing  $-df_s/d\phi_s$  with the function  $f_1(\phi_s)$ , marked by the broken curves in Figs. 13(a) and 13(b), determine the possible solutions of Eq. (5) for the surface volume fraction  $\phi_s$ .

For both the mixtures shown in Fig. 13 there appears only one solution for  $-df_s/d\phi_s = f_1(\phi_s)$  [Eq. (5)]. For each blend this solution is located at a value of  $\phi_s$  to the right of, and thus higher than the concentration of the second coexisting phase  $\phi_2$ . This would correspond to the complete wetting case of Fig. 1(b). The composition  $\phi_s > \phi_2$  at the intersection determines the small additional enrichment which decays rapidly to the composition  $\phi_2$  of the second coexisting phase [Fig. 1(b)]. For the case of the *d66/h52* blend, Fig. 13(a), the predicted complete wetting behavior by the *d66*-rich phase at the free surface at 184 °C, some 20 °C below the critical

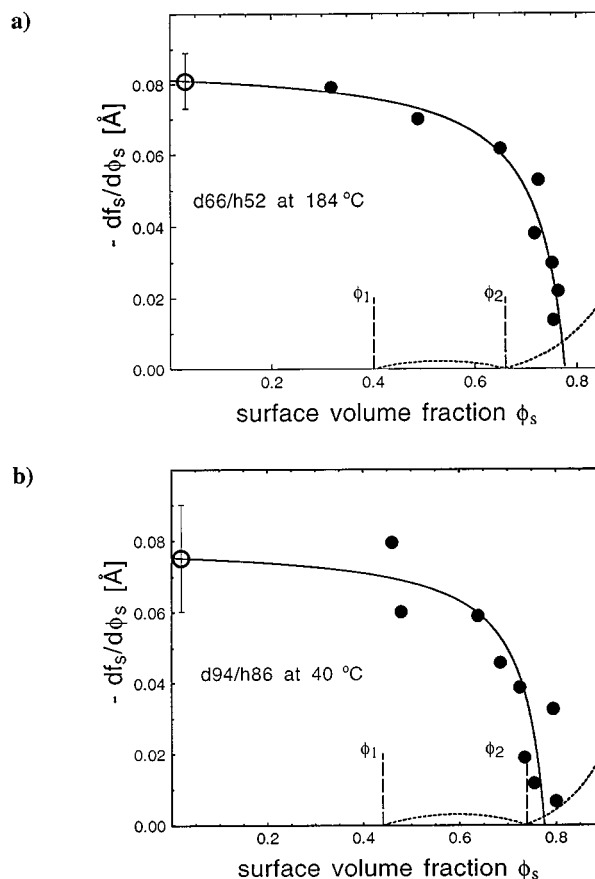


FIG. 13. Cahn constructions for the surface enrichment isotherms of the mixtures (a) *d66/h52* at 184 °C and (b) *d94/h86* at 40 °C. Points ● correspond to  $-df_s/d\phi_s$  based on the  $\phi_s$  vs  $\phi_\infty$  data in Fig. 12 (the open circles are based on an interpolation of the  $\phi_s$  vs  $\phi_\infty$  data between the  $\phi_s, \phi_\infty = 0$  datum and the lowest  $\{\phi_s, \phi_\infty\}$  data points in Fig. 12). The broken curves show the function  $f_1(\phi_s)$  from Eq. (6) for the region  $\phi_s > \phi_1$ , for the respective mixtures. The solid curves are fits based on the augmented surface potential [Eq. (11)],  $f_s^0(\phi_s) = -\mu_1\phi_s - \frac{1}{2}g\phi_s^2 - Y(d\phi/dz)_{z=0}$ , optimized with the following parameters:  
(a) *d66/h52*:  $\mu = 0.2$  Å,  $g = -0.26$  Å,  $Y = 4.1$  Å<sup>2</sup>  
(b) *d94/h86*:  $\mu = 0.19$  Å,  $g = -0.25$  Å,  $Y = 2.6$  Å<sup>2</sup>.

temperature for this blend, is fully consistent with the direct experimental observation of complete wetting by Steiner *et al.*<sup>9</sup> on the coexistence curve of the same blend at 150 °C. It is also consistent with the earlier observation of complete wetting at the polymer/air surface in the analogous mixture *d88/h78* at some 15 °C below the critical temperature. Finally, we note that, despite the greater scatter, complete wetting by the *d94*-rich phase at the air surface at 40 °C—some 10 °C below  $T_c$ —is also predicted for the *d94/h86* blend.

On the basis of our data, we may speculate concerning the expected order of the wetting transition. As the temperature of each mixture is lowered the broken curve representing  $f_1(\phi_s)$  shifts so that the positions of the coexisting compositions  $\phi_1$  and  $\phi_2$ , move out on the  $\phi_s$  axis to lower and higher values, respectively, while at the same time the “hump” between them becomes bigger. If  $df_s/d\phi_s$ —represented for each blend in Fig. 12 by the data points—were independent of temperature, then its intersection with  $f_1(\phi_s)$  would shift smoothly to lower and lower  $\phi_s$

values, in particular to  $\phi_s < \phi_2$ . This would imply a second order wetting transition on the coexistence curve. In practice, such an assumption about the temperature dependence of  $df_s/d\phi_s$  is *not* justified: the correct behavior, and its implication for the wetting transitions in such mixtures, is rather different and is explored in detail in our subsequent paper III<sup>38</sup> in this series.

#### D. The nature of the surface interactions

In his original discussion of critical point wetting<sup>1</sup> Cahn did not specify the precise form of the bare surface potential  $f_s(\phi_s)$ , except that it was local in the sense of being a function of  $\phi_s$  alone. Subsequently Schmidt and Binder, in their pioneering work on wetting transitions in polymer blends,<sup>5</sup> used a Taylor expansion in  $\phi_s$ , to order  $\phi_s^2$ , in order to describe this “bare” surface free energy

$$f_s = -\mu_1 \phi_s - \frac{1}{2}g \phi_s^2. \quad (9)$$

This simple form has been consistent with earlier<sup>19,20</sup> studies of surface enrichment from isotopic mixtures at low values of the bulk volume fraction. Qualitatively,  $\mu_1$  plays the role of a chemical potential difference favoring one of the components at the surface, while  $g$  represents the change of interactions near the surface (including the missing neighbors effect). More recently deviations from this form have been reported in a number of investigations,<sup>39,18</sup> indicating the limitations of this simple form for  $f_s$ . Clearly, also in the present study the simple linear form  $df_s/d\phi_s = -\mu_1 - g\phi_s$  implied by Eq. (9) does not describe well the data in Figs. 13(a) and 13(b).

Other extensions have been proposed to account for surface potentials in polymer mixtures beyond the virial expansion in Eq. (9). Short-ranged contributions of entropic origin have been noted earlier: they augment the bare surface energy expression with a term involving the composition gradient  $(d\phi/dz)_{z=0}$  at the surface. Both the Fredrickson–Donley [Eq. (2)] and the Cohen–Muthukumar treatments formulate the gradient term explicitly, but we have not been able to fit our experimental data using their expressions.<sup>40</sup>

Long-ranged surface interactions due to van der Waals forces may be accounted for<sup>2,10,11</sup> by adding a power-law term ( $\sim z^{-3}$ ) to the kernel of the integral defining the overall energy  $\Delta F$  [Eq. (3)], but the analysis leading to the Cahn construction is then no longer possible, and we have not pursued this line further. A recent calculation<sup>11</sup> suggests that the effect of long-ranged interactions of this sort on the composition profile may be rather weak.

Another approach, suggested both on general grounds<sup>4,41</sup> and in some more explicit models,<sup>42</sup> is to augment  $f_s$  by a term proportional to the composition gradient at the surface. This gives the modified form

$$f_s^a(\phi_s) = -\mu_1 \phi_s - \frac{1}{2}g \phi_s^2 - Y(d\phi/dz)_{z=0}. \quad (10)$$

Here we treat the parameter  $Y$  as adjustable and independent<sup>42</sup> of the volume fraction  $\phi$ .

We observe that adding a gradient term to the bare surface potential  $f_s$  allows us to describe our data rather well.<sup>43</sup>

To proceed, we note (as also observed in Ref. 18) the identity  $(d\phi/dz)|_{z=0} = (18/a^2)\phi_s(1-\phi_s)(df_s/d\phi_s)$ , which can be shown to follow<sup>4</sup> as the boundary condition resulting from minimization of  $F_s$  [Eq. (7)] with respect to  $\phi_s$ . Setting  $f_s = f_s^a$  and substituting this identity into Eq. (10), we find

$$(-df_s^a/d\phi_s) = [\mu_1 + g\phi_s]/[1 + (18/a^2)Y(1-2\phi_s)]. \quad (11)$$

Using this expression with three adjustable parameters  $\mu_1$ ,  $g$ , and  $Y$ ,  $(-df_s^a/d\phi_s)$  may be made to fit well to our data for  $(-df_s/d\phi_s)$  obtained from the experimental surface excess variation as described earlier. This is seen from the solid curves in Figs. 13(a) and 13(b); the best-fit values of these parameters are given in the caption to Fig. 13. Using the analytical form of  $f_s$ , together with Eqs. (5) and (6), we may back-calculate  $\phi_s(\phi_\infty)$  and, using Eq. (8) we may then back-calculate  $\Gamma(\phi_\infty)$ . These back-calculated values are shown, respectively, as the solid curves in Fig. 11, and in Figs. 9 and 10. The fits are good, indicating the internal consistency of our procedure; the calculated values of  $\Gamma(\phi_\infty)$  in particular show a divergence of the surface excess as  $\phi_\infty$  approaches the coexistence value  $\phi_1$ . We conclude that a form for the surface potential  $f_s$ , modified relative to the simple two-term expression by adding a term in the composition gradient at the surface, can account well for our data.

#### V. SUMMARY AND CONCLUSIONS

The surface enrichment from 12 binary mixtures of poly( $E_{1-x}E_x$ ) random copolymers has been measured both at the polymer/air and at two polymer/solid surfaces, at mixture compositions and temperatures in the one-phase regime of the coexistence diagram. Critical temperatures and bulk segmental interactions in these mixtures were determined in our earlier paper (I). We find that in all cases the component with the higher ethyl branching ratio, i.e., the higher  $x$  value, corresponding to a lower statistical segment length, is favored at the air surface, but that—within our resolution—neither component is enriched at the polymer/solid interfaces. This suggests that the driving potential for the surface enrichment is predominantly enthalpic, rather than entropic, in origin. A study of the surface excess of the enriched components from two of the mixtures, at several mixture compositions along an isotherm in the one-phase regime, enables analysis of our data in terms of a mean-field model and the Cahn construction. The findings are consistent with our earlier observations of complete wetting on the coexistence curve from the same or similar  $E/EE$  mixtures. Our results may be rather well fitted using a form of the surface potential which includes a term in the mixture composition *gradient* at the surface, in addition to terms in the surface composition itself. A more detailed discussion of the wetting transition from such model polymer blends requires knowledge of the surface enrichment as a function of temperature as well of mixture composition, and is described in paper III<sup>38</sup> of this series.

## ACKNOWLEDGMENTS

We thank Jakub Rysz and Tobias Kerle for their help. Useful discussions with David Lohse, Rocco Jerry and especially with Kurt Binder are acknowledged with appreciation. We also thank the German-Israel Foundation (G.I.F.), the U.S.-Israel Binational Science Foundation (BSF), the Commission of the European Communities, the Minerva Foundation, and the Ministry of Sciences and Arts (Israel) for their support of this work.

- <sup>1</sup>J. W. Cahn, *J. Chem. Phys.* **66**, 3667 (1977).
- <sup>2</sup>P.-G. de Gennes, *Rev. Mod. Phys.* **57**, 827 (1985).
- <sup>3</sup>M. Schick, in *Les Houches, session XLVIII, Liquids at Interfaces*, edited by J. Charvolin, J. F. Joanny, and J. Zinn-Justin (North-Holland, Amsterdam, 1990), pp. 419–497.
- <sup>4</sup>K. Binder, *Acta Polym.* **46**, 204 (1995).
- <sup>5</sup>I. Schmidt and K. Binder, *J. Phys. (Paris)* **46**, 1631 (1985).
- <sup>6</sup>U. Steiner, J. Klein, E. Eiser, A. Budkowski, and L. J. Fetters, in *Ordering in Macromolecular Systems*, edited by A. Teramoto (Springer, Berlin, 1994), pp. 313–329.
- <sup>7</sup>H. Nakanishi and P. Pincus, *J. Chem. Phys.* **79**, 997 (1983).
- <sup>8</sup>U. Steiner, J. Klein, E. Eiser, A. Budkowski, and L. J. Fetters, *Science* **258**, 1126 (1992).
- <sup>9</sup>U. Steiner, J. Klein, and L. J. Fetters, *Phys. Rev. Lett.* **72**, 1498 (1994).
- <sup>10</sup>Z. Y. Chen, J. Noolandi, and d. Izzo, *Phys. Rev. Lett.* **66**, 727 (1991).
- <sup>11</sup>R. A. L. Jones, *Phys. Rev. E* **47**, 1437 (1993).
- <sup>12</sup>S. M. Cohen and M. Muthukumar, *J. Chem. Phys.* **90**, 5749 (1989).
- <sup>13</sup>G. H. Fredrickson and J. P. Donley, *J. Chem. Phys.* 8941 (1992).
- <sup>14</sup>J. P. Donley and G. H. Fredrickson, *J. Polym. Sci., Part B* **33**, 1343 (1995).
- <sup>15</sup>G. H. Fredrickson and A. J. Liu, *J. Polym. Sci., Part B* **33**, 1203 (1995).
- <sup>16</sup>Q. S. Bhatia, D. H. Pan, and J. T. Koberstein, *Macromolecules* **21**, 2166 (1988).
- <sup>17</sup>F. Bruder and R. Brenn, *Phys. Rev. Lett.* **69**, 624 (1992).
- <sup>18</sup>F. Bruder and R. Brenn, *Europhys. Lett.* **22**, 707 (1993).
- <sup>19</sup>R. L. Jones, E. J. Kramer, M. H. Rafailovich, J. Sokolov, and S. A. Schwarz, *Phys. Rev. Lett.* **62**, 280 (1989).
- <sup>20</sup>A. Budkowski, U. Steiner, and J. Klein, *J. Chem. Phys.* **97**, 5229 (1992).
- <sup>21</sup>U. Steiner, J. Klein, E. Eiser, A. Budkowski and L. J. Fetters, *Ber. Bunsenges. Phys. Chem.* **98**, 366 (1994).
- <sup>22</sup>F. Scheffold, E. Eiser, A. Budkowski, U. Steiner, J. Klein, and L. J. Fetters, *J. Chem. Phys.* **104**, 8786 (1996) (preceding paper in this issue).
- <sup>23</sup>U. K. Chaturvedi, U. Steiner, O. Zak, G. Krausch, G. Schatz, and J. Klein, *Appl. Phys. Lett.* **56**, 1228 (1990).
- <sup>24</sup>J. Klein, *Science* **250**, 640 (1990).
- <sup>25</sup>We use the root mean square deviation  $\sigma$  of a Gaussian distribution in order to characterize the system resolution. This measure relates to the half width at half maximum (HWHM)  $w$  of a step function as  $w = (2 \ln 2)^{1/2} \sigma = 1.177 \sigma$ .
- <sup>26</sup>W.-K. Chu, J. W. Mayer, and M.-A. Nicolet, *Backscattering Spectrometry* (Academic, New York, 1978).
- <sup>27</sup>A. Losch, F. Scheffold, U. Steiner, T. Kerle, G. Schatz, and J. Klein (unpublished).
- <sup>28</sup>T. Flebbe, D. Burkhard, and K. Binder (unpublished).
- <sup>29</sup>In some cases surface nucleated spinodal decomposition resulted in a small depletion layer adjacent to a large surface peak. This was corrected for by subtracting the area of the depletion layer from the total area of the surface layer.
- <sup>30</sup>R. Krishnamoorti, W. W. Graessley, N. P. Balsara, and D. J. Lohse, *Macromolecules* **27**, 3073 (1994).
- <sup>31</sup>M. Sikkah, N. Singh, A. Karim, F. S. Bates, S. K. Satija, and C. F. Majkrzak, *Phys. Rev. Lett.* **70**, 307 (1993).
- <sup>32</sup>M. A. Carignano and I. Szleiffer, *Europhys. Lett.* **30**, 525 (1995).
- <sup>33</sup>We did not have sufficient independent information on the surface parameters of our mixtures (e.g., differences in surface tension of the different components) for a detailed comparison with the criterion for entropic vs enthalpic dominance given in Ref. 13. A comparison based on the parameter  $\mu_1$  extracted from our data via the Cahn construction [see Eqs. (9)–(11) and caption to Fig. 13] suggests the enthalpic term is dominant.
- <sup>34</sup>See computer simulations by K. P. Walley, K. S. Schweizer, J. Peanasky, L. Cai, and S. Granick, *J. Chem. Phys.* **100**, 3361 (1994) and references to earlier work therein.
- <sup>35</sup>P. G. deGennes, *J. Chem. Phys.* **72**, 4756 (1980).
- <sup>36</sup>P. Flory, *Principles of Polymer Chemistry* (Cornell University Press, Ithaca, NY, 1971); P. G. de Gennes, *Scaling Concepts in Polymer Physics* (Cornell University Press, Ithaca, N.Y., 1979).
- <sup>37</sup>We note a word of caution that determination of  $\phi_s$  via neutron reflectometry (J. Genzer, A. Faldi, R. Oslanec, and R. Composto—preprint) shows some discrepancy with values of  $\phi_s$  either measured using the surface excess approach, or expected from the mean-field expression (8).
- <sup>38</sup>A. Budkowski, F. Scheffold, U. Steiner, J. Klein, and L. J. Fetters (unpublished).
- <sup>39</sup>X. Zhao, W. Zhao, J. Sokolov, M. H. Rafailovich, S. A. Schwarz, B. J. Wilkens, R. A. L. Jones, and E. J. Kramer, *Macromolecules* **24**, 5991 (1991).
- <sup>40</sup>In the case of the Fredrickson–Donley model, the prefactor of the  $(d\phi/dz)_{z=0}$  term, Eq. (2), is too small by about an order of magnitude to account for the observed variation of  $df_s/d\phi_s$ . In an earlier study of surface segregation from a polystyrene/brominated-polystyrene mixture (Ref. 18), the Cohen–Muthukumar model was used to account for data showing a *downturn* in surface excess as the mixture composition approached the coexistence curve in the one-phase regime.
- <sup>41</sup>K. Binder (private communication).
- <sup>42</sup>R. A. Jerry and E. B. Nauman, *J. Colloid Interface Sci.* **154**, 122 (1992); *Phys. Rev. E* **48**, 1583 (1993). In this model [which includes also terms in  $(d^2\phi/dz^2)$ ] the parameter  $Y$  [Eq. (10)] is a function of the intermolecular interactions of the mixture components and is independent of the mixture composition  $\phi$ .
- <sup>43</sup>Adding to  $f_s$  a third virial term in  $\phi_s^3$ , say, which is a natural extension to the virial expression for  $f_s$  in Eq. (9), cannot account for the slow, quasi-linear decrease of  $df_s/d\phi_s$  (data points in Fig. 13) at  $\phi_s < 0.6$  followed by the sharp downturn at higher  $\phi_s$ .